Available online at www.sciencedirect.com
ScienceDirect
Journal of Sound and Vibration 324 (2009) 26–39
JOURNAL OF SOUND AND VIBRATION
www.elsevier.com/locate/jsvi

Optimized chatter resistance of viscoelastic turning bars

J. Saffury*, E. Altus

Faculty of Mechanical Engineering, Technion, Israel Institute of Technology, Haifa 32000, Israel

Received 15 September 2008; received in revised form 7 January 2009; accepted 4 February 2009
Handling Editor: C.L. Morfey
Available online 12 March 2009

Abstract

The regenerative-chatter resistance of a viscoelastic cantilever beam is analyzed and compared to the common dynamic vibration absorber (DVA) system. The beam represents a tool holder for turning operation in machining. The optimum structural parameters are found by maximizing the most negative real part of the frequency response function (FRF). The FRF is found analytically by using an appropriate Green's function. Keeping the cantilever static stiffness constant, further increase in the optimal resistance is achieved by changing the ratio between the two elastic moduli in the 3-parameter solid viscoelastic material model. Three additional chatter resistance indicators are also investigated: the most positive real part of the FRF, the magnitude of the FRF and the resonant frequency. It is found that in contrast to the DVA system, the chatter resistance of the viscoelastic beam is optimal with respect to the above indicators for approximately unique set of the same material parameters.

1. Introduction

One of the common operations in machining is creating cylindrical deep holes by single-point turning. The cutting tool holder is usually a cantilever with cylindrical cross-section and large overhang ratio (length to diameter "L/D"). The deflection and vibration response limit the allowable machining conditions. Usually, with an overhang ratio $L/D>4$, vibration instabilities, known as chatter, become apparent. The chatter causes a noticeable wear in the cutting tool and limits machining productivity since the cutting removal rate is usually reduced. Chatter vibrations increase surface roughness, reduce machining accuracy and produce an irritating unacceptable noise.

Regenerative and non-regenerative chatters are two types of machine tool chatters. Regenerative chatter results from cutting on a previous wavy surface and non-regenerative chatter occurs in some special conditions such as mode coupling. In this article we will focus on the regenerative chatter which is the most common type occurring in turning operations (Wang and Fei [1], Tlusty [2], Pratt and Nayfeh [3], Chen and Tsao [4]).

Enhancing the chatter resistance and therefore increasing allowable overhang ratio of tool holders is achieved by active (e.g. Takemura et al. [5], Pratt and Nayfeh [6]) and passive methods (e.g. Tobias [7], Rivin and Kang [8]). Despite the potential advantages of active methods, passive methods remain a useful device for

*Corresponding author. Tel.: +972 546 800283; fax: +972 777 808703.
E-mail address: saffury@tx.technion.ac.il (J. Saffury).

0022-460X/$ - see front matter © 2009 Elsevier Ltd. All rights reserved.
doi:10.1016/j.jsv.2009.02.004

Nomenclature

b	chip width
c	DVA normalized modal damping
E_1, E_2	elastic moduli in the 3-parameter solid viscoelastic material model
f	DVA normalized eigen-frequency
$G_{x\zeta t\tau}$	Green's function as a function of x, ζ, t and τ
$G_1(i\omega)$	frequency response function
h	chip thickness
k	DVA normalized modal stiffness
m	DVA normalized mass
u_1, u_2	orientation coefficients
u_{xt}	beam transverse displacement at x location and time t
y	displacement of the cutting tool normal to the cut surface
Y	relaxation modulus
ε	relative phase angle of vibration between successive tooth passes
η	damping ratio of the viscoelastic beam
ξ	DVA damping ratio
ψ	frequency parameter
ω	vibration angular frequency

Notations

$Z_{x_1x_2\ldots x_n}$	a function Z of n independent variables x_1, x_2,…,x_n (i.e. $Z(x_1,x_2,\ldots,x_n)$)
$Z_{x_1x_2\ldots x_n,x_ix_j\ldots x_k}$	partial derivatives of $Z_{x_1x_2\ldots x_n}$ with respect to x_i, x_j,…,x_k (i, j, $k = 1,2,3,\ldots$)
$\bar{F}_s$	Laplace transform of F_t with respect to time (t)
Re(F)	real part of a complex function F
Abs(F)	magnitude of a complex function F

improving the chatter stability of machining systems, due to their lower complexity and cost. Several passive methods have been studied in the literature: (1) anisotropic bars (Thomas et al. [9]), proved experimentally by Mescheriakov et al. [10] to be hardly possible to implement; (2) bars made of high Young's modulus material such as sintered tungsten carbide (Rivin and Kang [8], Nagano et al. [11]); (3) bars with viscoelastic clamping device (Rivin and Kang [12]); (4) a dynamic vibration absorber (DVA) attached to the bar (Fig. 1(a)) (e.g. Donies and Van Den Noortgate [13]). The DVA has to be placed inside the tool holder in an internal cavity and at the furthest available position and (5) a "combination structure" (Rivin [14], Rivin and Kang [8]), which is a heterogeneous bar made from two parts: a root segment (with high Young's modulus) and an overhanging free segment (made of light material). This design improves the effect of an attached DVA by increasing the mass ratio.

The common DVA device, when tuned to the proper frequency, can reduce the peak magnitude of the frequency response function (FRF) of the tool holder. This is achieved by using Ormondroyd and Den Hartog's classical "equal peaks" method (Den Hartog [15]). However, for improving the chatter stability other methods have been proposed: analytical solutions (Rivin and Kang [8], Sims [16]), numerical optimized solutions using machining simulations (Liu and Rouch [17]) and manual tuning (Tarng et al. [18]).

The main disadvantage of passive vibration absorbers is the need for adaptive tuning during machining, e.g. if the sign of an "orientation factor" changes because of a change in the cutting conditions the DVA has to be

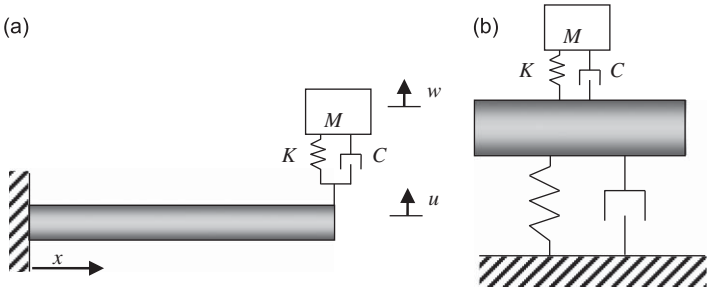

Fig. 1. (a) A typical dynamic vibration absorber attached to a cantilever tool holder and (b) equivalent lumped mass model.

tuned accordingly. In addition, the DVA performance is limited by the need to place it on the cutting tool without interfering with the cutting process.

Analytical solutions of stability limit in turning show that the depth of cut dominates the chatter instability and is inversely proportional to the most negative real value of the FRF (Tlusty [2]). The analysis introduced by Rivin and Kang [8] and Sims [16], considers the cantilever tool as a lumped, linear and one degree of freedom (dof) model. The DVA is considered as an additional linear dof. Rivin [19] used the $K\delta$ optimization criteria, where K is the effective stiffness and δ represents the log-decrement damping parameter of the cantilever with the DVA. Sims introduced three different optimizations: minimizing the peak magnitude of the FRF, maximizing the most negative real part of the FRF and minimizing the most positive real part of the FRF. Although Rivin's method offers superior performance over Den Hartog's method, Sims stated that it does not optimize the most negative or most positive real parts of the FRF.

To our knowledge, optimization of viscoelsatic beams (VB) as turning bars and comparison with a corresponding DVA system have not been fully investigated yet, in particular with regard to optimization of chatter resistance. In this work, the cantilever tool is modeled as a continuous beam made from a uniform linear viscoelastic material. Practically, viscoelastic behavior of a beam can be achieved by using several methods such as the Fluid Surface Damping and constrained layer damping techniques (Ghoneim [20]). In the analysis of the present article, the cantilever transverse displacement is only considered although rotation and axial displacements may also occur. The transversal stiffness at the cantilever tip is proportional to D^4/L^3 while the rotational and axial ones are proportional to D^4/L and D^2/L, respectively. Therefore, an increase in L/D decreases considerably the transversal stiffness with respect to the rotational and axial ones. The significance of the rotational stiffness is demonstrated in Rivin and Kang [8] work for turning at high cutting speeds.

The optimization criteria used in this study is based on the most negative real part of the FRF. In addition the optimal response is also examined by comparing the other two indicators: the most positive real part and the peak magnitude of the FRF. The effect of the tuning on the resonant frequency is studied too. The VB holder is also compared to elastic continuous cantilever with a tuned DVA (CDVA) attached to its tip. In this work, Sims method for tuning a DVA attached to a lumped mass model is generalized to the CDVA model.

2. Theory

In turning processes, three main types of vibrations may occur: free, forced and self-excited. The free vibration is transient and less important than the forced and self-excited ones. Forced vibrations arise with the application of periodic cutting forces acting on the cutting tool. Forced vibrations magnitude become large when a cutting force frequency approaches the natural frequency of the cutting tool (resonance). Self-excited vibrations result from an interaction between the cutting forces and cutting edge displacements. The amplitude of self-excited vibrations increases rapidly up to some amplitude which is limited by the nonlinearity of the cutting process. The frequency of self-excited vibrations is close to and greater than the natural frequency of the cantilever tool (Tlusty [2]).

Tlusty and Polacek [21] introduced a simplified beam model for regenerative chatter analysis for turning operations as shown in Fig. 2. The system of workpiece and cutting tool are linear and characterized by two individual modes of vibration (directions x_1 and x_2). Vibration amplitudes y_0 and y represent the wavy surfaces, before and after a cutting pass, respectively, with a phase shift (ε). The cutting force F is assumed directly proportional to the chip area and has a constant direction β.

The process of self-excitation is a closed loop in which the tool vibration induces a force variation, which in turn affects the tool vibrations. The feedback relationship of vibrations y caused by force variation F' is in general: $y = G_0(i\omega)F'$. The oriented transfer function (TF) G_0 can be represented as a sum of the direct TFs G_i of uncoupled modes in x_i directions multiplied by the "orientation factors" (u_i), i.e. $G_0 = u_i G_i$. It is shown in Ref. [2] that the chip width (b) at the stability limit point is

$$b_{\lim} = \frac{-1}{2K_s \mathrm{Re}(G_0(i\omega))}. \tag{2.1}$$

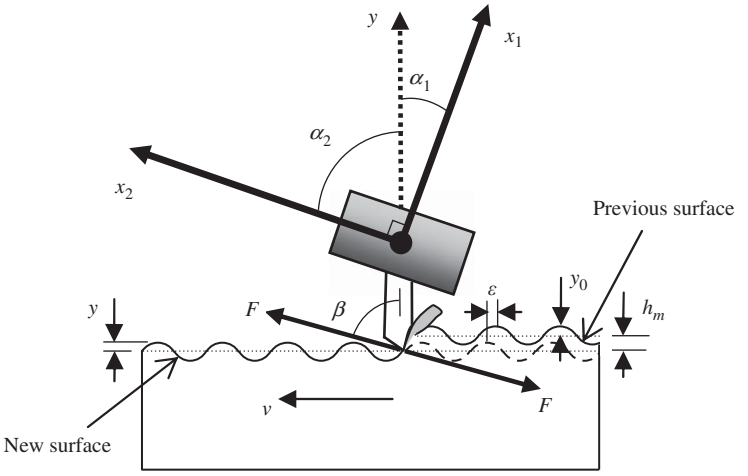

Fig. 2. The regeneration diagram relating force, surface waviness and vibration.

K_s (N/m^2) is the "specific force", that is, force per unit chip area and within a first approximation it is a workpiece material constant (K_s values for selected materials are given in Ref. [2]).

The smallest chip width at which chatter may occur is

$$b_{\mathrm{lim,cr}} = \frac{-1}{2K_s \min(\mathrm{Re}(G_0(\mathrm{i}\omega)))}, \tag{2.2}$$

where $\min(\mathrm{Re}(G_0(\mathrm{i}\omega)))$ denotes the most negative (minimum) real part of $G_0(\mathrm{i}\omega)$.

Cutting is stable when $b < b_{\mathrm{lim,cr}}$ and chatter is developed when $b > b_{\mathrm{lim,cr}}$. Eq. (2.2) has great practical significance and is used to analyze and design optimal cutting tools. It offers a clear criterion for the dynamic response of the machine–tool interaction.

3. Chatter resistance optimization

In this work, the cantilever holder is assumed to be made of linear viscoelastic material. For simplicity, the cantilever cross-section orientation (determined by α_i) is chosen such that one of the orientation factors (say u_2) is neglected. Assuming $u_1 > 0$, (2.2) becomes

$$b_{\mathrm{lim,cr}} = \frac{-1}{2K_s u_1 \min(\mathrm{Re}(G_1(\mathrm{i}\omega)))}, \tag{3.1}$$

then it is desirable to increase $\min(\mathrm{Re}(G_1(\mathrm{i}\omega)))$. Note that if $u_1 < 0$, the chatter stability is dictated by the most positive real part of $G_1(\mathrm{i}\omega)$ ($\max(\mathrm{Re}(G_1(\mathrm{i}\omega)))$) which should be decreased for increasing $b_{\mathrm{lim,cr}}$.

In this study, we find $G_1(\mathrm{i}\omega)$ by transferring the impulse response function (Green's function) of the cantilever problem into the Laplace domain (Karnovsky and Lebed [22]).

The dynamic governing equation of a uniform VB with a cross-section A, density ρ, viscoelastic modulus Y and inertia I, loaded by a distributed load q_{xt} is

$$(Y_{tt'} \underset{t'}{*} u_{xt',xxt'} I)_{,xx} + \rho A u_{xt,tt} = q_{xt}; \quad 0 < x < L, \ \ t > 0. \tag{3.2}$$

The boundary conditions (BCs) are

$$u_{xt}|_{x=0} = u_{xt,x}|_{x=0} = u_{xt,xx}|_{x=L} = u_{xt,xxx}|_{x=L} = 0; \quad t > 0. \tag{3.3}$$

The operation $P_{tt'} \underset{t'}{*} Q_{t',t'}$ between two functions $P(t)$ and $Q(t)$, denotes the hereditary integral (Flügge [23]):

$$P_{tt'} \underset{t'}{*} Q_{t',t'} \equiv P(t) \cdot Q(0) + \int_{t'=0}^{t} P(t-t') \cdot \frac{\partial Q(t')}{\partial t'} \, \mathrm{d}t' \tag{3.4}$$

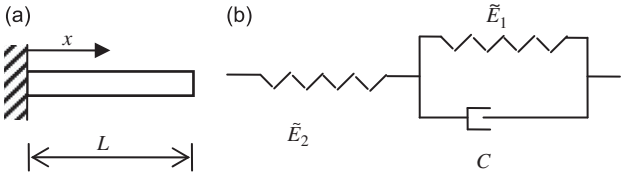

Fig. 3. (a) A cantilever beam model and (b) 3-parameter solid model of a linear viscoelastic material.

and x is the distance from the fixed end (Fig. 3(a)). Green's function is the solution of the boundary value problem (BVP) (3.2) and (3.3) for impulse loading, i.e.

$$(Y_{tt'} \underset{t'}{*} G_{x\zeta t'\tau,xxt'I})_{,xx} + \rho A G_{x\zeta t\tau,tt} = \delta(x-\zeta)\delta(t-\tau); \quad 0<x,\ \zeta<L;\ \ t,\ \tau>0. \tag{3.5}$$

The BCs are similar to Eq. (3.3). For stationary BVP,

$$G(x,\zeta,t,\tau) = G(x,\zeta,t-\tau) = G(x,\zeta,\Delta t). \tag{3.6}$$

The Laplace transform of the Green's function $G(x, \zeta, \Delta t)$ with respect to Δt, is the TF of the beam problem and it is the solution of the following static BVP:

$$(s\bar{Y}_s\bar{G}_{x\zeta s,xx}I)_{,xx} + \rho A s^2 \bar{G}_{x\zeta s} = \delta(x-\zeta); \quad 0<x,\ \ \zeta<L, \tag{3.7}$$

with BCs,

$$\bar{G}_{x\zeta s}|_{x=0} = \bar{G}_{x\zeta s,x}|_{x=0} = \bar{G}_{x\zeta s,xx}|_{x=L} = \bar{G}_{x\zeta s,xxx}|_{x=L} = 0. \tag{3.8}$$

The solution of Eqs. (3.7) and (3.8) is as follows: divide the beam's length into two regions: $x<\zeta$ and $x>\zeta$. In each region solve Eq. (3.7) with the RHS = 0. Then apply the BCs (3.8) and the continuity conditions:

$$\bar{G}_{x\zeta s}|_{x=\zeta^+} = \bar{G}_{x\zeta s}|_{x=\zeta^-}; \quad \bar{G}_{x\zeta s,x}|_{x=\zeta^+} = \bar{G}_{x\zeta s,x}|_{x=\zeta^-};$$

$$\bar{G}_{x\zeta s,xx}|_{x=\zeta^+} = \bar{G}_{x\zeta s,xx}|_{x=\zeta^-}; \quad \bar{G}_{x\zeta s,xxx}|_{x=\zeta^+} - \bar{G}_{x\zeta s,xxx}|_{x=\zeta^-} = \frac{1}{s\bar{Y}_s I}. \tag{3.9}$$

Recall that the model represents a tool holder with a cutting force applied at the tip so that $\bar{G}_{x\zeta s}|_{x=\zeta=L}$ is our main interest. The solution of Eqs. (3.7) and (3.8) at $x=\zeta=L$ and with s = iω (ω is an angular frequency) is obtained analytically:

$$\bar{G}_{x\zeta\omega}|_{\substack{x=L\\ \zeta=L}} = \frac{\theta}{L\omega^2\rho A}\cdot\frac{\sin(\theta)\cosh(\theta)-\cos(\theta)\sinh(\theta)}{1+\cos(\theta)\cosh(\theta)}, \tag{3.10}$$

where θ is defined by

$$\theta^4 \equiv \frac{\omega^2\rho A L^4}{I(s\bar{Y}_s)|_{s=\mathrm{i}\omega}}. \tag{3.11}$$

Finally, we use the equality:

$$\bar{G}_{x\zeta\omega}|_{\substack{x=L\\ \zeta=L}} = G_1(\mathrm{i}\omega). \tag{3.12}$$

For a 3-parameter solid viscoelastic model (Fig. 3(b)),

$$(s\bar{Y}_s)|_{s=\mathrm{i}\omega} = \frac{\tilde{E}_2(\tilde{E}_1+\mathrm{i}\omega C)}{\tilde{E}_1+\tilde{E}_2+\mathrm{i}\omega C}. \tag{3.13}$$

Defining E as an equivalent Young's modulus when $C\to 0$, (3.10) and (3.12) yield:

$$G_1(\mathrm{i}\omega) = \frac{\alpha L^3}{EI\psi^4}\cdot\frac{\sin(\alpha)\cosh(\alpha)-\cos(\alpha)\sinh(\alpha)}{1+\cos(\alpha)\cosh(\alpha)}; \quad \alpha \equiv \frac{\psi}{Z_\psi}. \tag{3.14}$$

ψ is a frequency parameter and Z_ψ is related to the relaxation modulus as

$$\psi^4 \equiv \frac{\omega^2 \rho A L^4}{EI}; \quad Z_\psi^4 \equiv \frac{E_2(E_1 + 2\mathrm{i}\psi^2\eta)}{E_1 + E_2 + 2\mathrm{i}\psi^2\eta}. \tag{3.15}$$

E_1 and E_2 are normalized Young moduli and η is a damping ratio:

$$E_1 \equiv \frac{\tilde{E}_1}{E}; \quad E_2 \equiv \frac{\tilde{E}_2}{E}; \quad \eta \equiv \frac{C}{2}\sqrt{\frac{I}{E\rho A L^4}}. \tag{3.16}$$

Normalizing $G_1(\mathrm{i}\omega)$ in Eq. (3.14) by the static deflection ($G_1(0)$), we use a normalized form without re-notation:

$$G_1(\mathrm{i}\omega) = \frac{3\alpha}{\psi^4}\left(\frac{E_1 E_2}{E_1 + E_2}\right)^4 \frac{\sin(\alpha)\cosh(\alpha) - \cos(\alpha)\sinh(\alpha)}{1 + \cos(\alpha)\cosh(\alpha)}. \tag{3.17}$$

$\min(\mathrm{Re}(G_1(\mathrm{i}\omega)))$ which controls the stability against regenerative chatter (3.1) will be optimized as follows.

Let us expose the main characteristics of the solution by considering an example where $E_1 = E_2 = 2$ and various η values as seen in Fig. 4. The specific values of E_i are chosen such that the effective modulus is 1 for $\eta = 0$. For very small or very large values of η, $\min(\mathrm{Re}(G_1(\mathrm{i}\omega)))$ approaches $-\infty$, which indicates that chatter will always occur even for a very small value of b. However, for intermediate values of η, the minimum point and therefore $b_{\mathrm{lim,cr}}$ are finite.

Fig. 4 shows two damping-independent (locked) points. Therefore $\min(\mathrm{Re}(G_1(\mathrm{i}\omega)))$ is constrained by these points. The frequency parameters of the "positive" and "negative" locked-points, denoted by $\psi^{(\mathrm{p})}$ and $\psi^{(\mathrm{n})}$, are equal to the cantilever eigen-parameters when $\eta \to 0$ and $\eta \to \infty$, respectively. Optimal value of $\min(\mathrm{Re}(G_1(\mathrm{i}\omega)))$ is obtained for η which exhibits a minimum at $\psi^{(\mathrm{n})}$ (i.e. for $\eta \cong 0.4$). The condition at this point is

$$\left.\frac{\mathrm{d}\,\mathrm{Re}(G_1(\mathrm{i}\omega))}{\mathrm{d}\psi}\right|_{\psi=\psi^{(\mathrm{n})}} = 0. \tag{3.18}$$

The optimum can be further improved by choosing different E_1/E_2 ratios, keeping the cantilever static stiffness ($\mathrm{Re}(G_1(\mathrm{i}\omega)$ when $\psi \to 0$) the same. Comparison between three E_1/E_2 ratios at the associated optimal responses

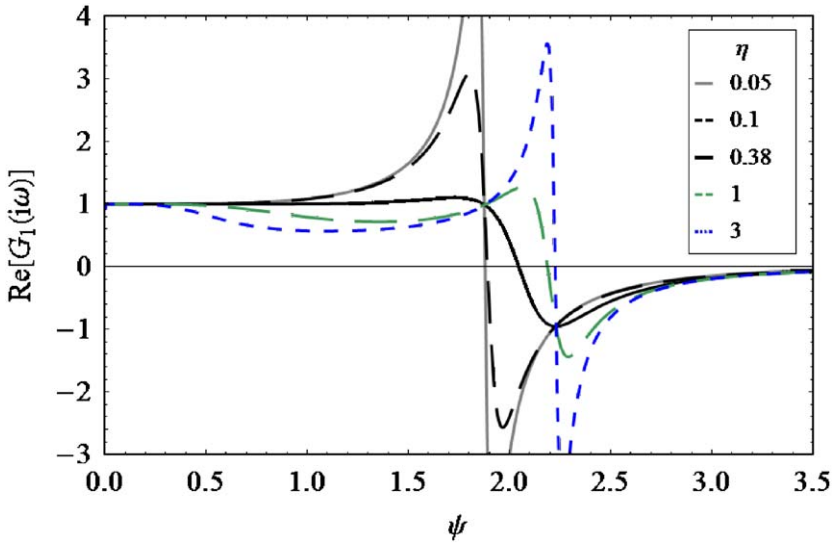

Fig. 4. The frequency response function real part, for a viscoelastic cantilever with $E_1 = E_2 = 2$ and various values of the damping ratio η. There are two locked-points.

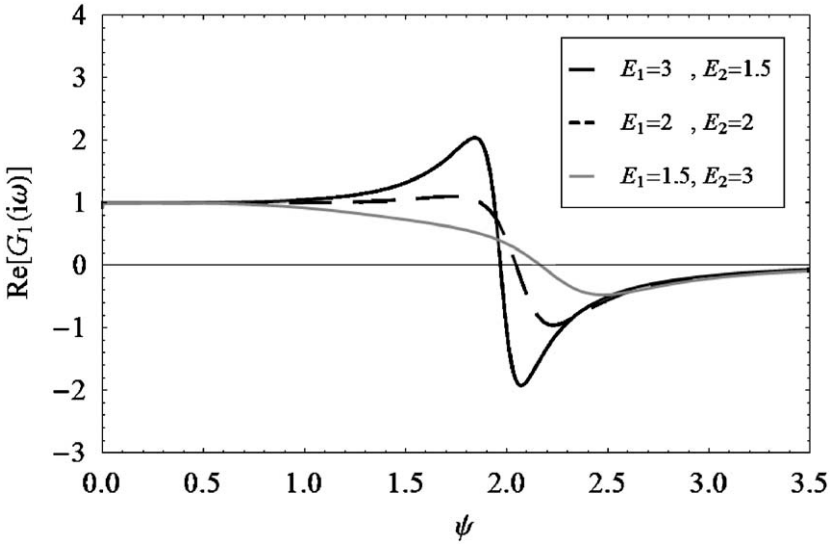

Fig. 5. The frequency response function real part for the optimized viscoelastic cantilever, at three different E_1/E_2 ratios. Static stiffness is similar.

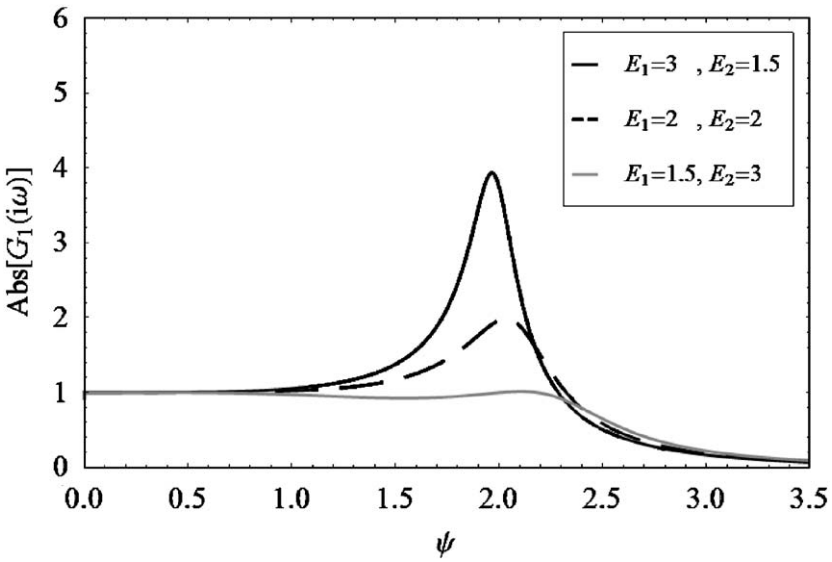

Fig. 6. The frequency response function magnitude for the optimized viscoelastic cantilever, at three different E_1/E_2 ratios. Static stiffness is similar.

is shown in Fig. 5. It can be seen that by changing E_1/E_2 from 2 to 1/2, $b_{\mathrm{lim,cr}}$ is increased by three-fold. In addition, improving the optimum is followed by an increase in both the chatter and the resonance frequencies (see Figs. 5 and 6). The system is therefore more stable (Szuba et al. [24], Yen and Hsueh [25], Rivin and Kang [8]).

4. Sims optimization method for an elastic continuous beam model with an attached DVA (CDVA)

In this section, Sims [16] method for tuning a DVA attached to a lumped mass model is generalized to a CDVA model (Fig. 1). The FRF of the CDVA at the tip will be obtained explicitly. The most negative or

positive real parts of the FRF will be optimized. The DVA parameters at the optimum for the two models will be compared. It will be shown that the results of the two models are essentially identical.

The FRF of a uniform elastic cantilever with a DVA attached to its tip was obtained analytically by Korenev and Reznikov [26]. After some algebraic manipulations the FRF at the cantilever tip ($G_1(i\omega)$), normalized by $G_1(0)$ (without re-notation), is

$$G_1(i\omega) = \frac{3}{\dfrac{m\psi^4(k + ic\psi^2)}{m\psi^4 - ic\psi^2 - k} + \sigma_\psi}. \tag{4.1}$$

m, c, k are normalized DVA modal parameters defined by

$$m \equiv \frac{M}{L\rho A}; \quad c \equiv C\sqrt{\frac{L^2}{EI\rho A}}; \quad k \equiv K\frac{L^3}{EI}. \tag{4.2}$$

E is the Young modulus of the cantilever and σ_ψ is defined by

$$\sigma_\psi = \psi^3 \frac{1 + \cos(\psi)\cosh(\psi)}{\cosh(\psi)\sin(\psi) - \cos(\psi)\sinh(\psi)}, \tag{4.3}$$

which represents the contribution of the elastic cantilever to $G_1(i\omega)$.

Following Sims' method, we first obtain the damping invariant points of the response. Fig. 7 shows the response of the CDVA system for $m = 0.1$ and different c and k values in the vicinity of $\psi^{(1)}$, which is the first eigen-parameter of an elastic cantilever beam without DVA ($\psi^{(1)} \cong 1.8751$). Three points are invariant (locked) to the damping ratio c. These points are essential in this tuning method and can be obtained by finding the roots of the denominator of $\mathrm{Re}(G_1(i\omega))$ at $c = 0$ and at $c \to \infty$. For $c = 0$ and given values of m and k, two roots near $\psi^{(1)}$ can be obtained from Eq. (4.1):

$$\sigma_\psi + \frac{km\psi^4}{m\psi^4 - k} = 0. \tag{4.4}$$

These roots are denoted by $\psi^{(p)}$ and $\psi^{(n)}$ ($\mathrm{Re}(G_1(i\omega))$ is positive at $\psi^{(p)}$ and negative at $\psi^{(n)}$). For $c \to \infty$ the third root (denoted by $\psi^{(a)}$) of the denominator, can be obtained by the equation:

$$\sigma_\psi - m\psi^4 = 0. \tag{4.5}$$

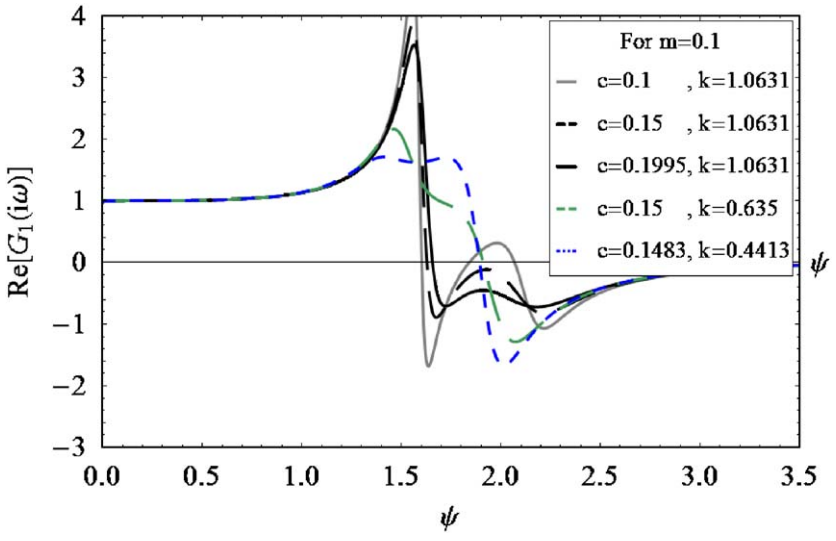

Fig. 7. The frequency response function real part, for a cantilever with DVA system.

In this tuning method, for optimizing max(Re(G_1(iω))), one equates Re(G_1(iω)) at $\psi = \psi^{(a)}$ to Re(G_1(iω)) at $\psi = \psi^{(p)}$, then requires that Re(G_1(iω)) at $\psi^{(p)}$ or $\psi^{(a)}$ has a maximum. These two optimum conditions determine both c and k for every given value of m. For optimizing min(Re(G_1(iω))), one equates Re(G_1(iω)) at $\psi^{(a)}$ to Re(G_1(iω)) at $\psi^{(n)}$, then requires that Re(G_1(iω)) at $\psi^{(p)}$ or $\psi^{(a)}$ has a minimum. This optimization procedure is based on Sims' method [16], where Den Hartog's "equal peaks" method is adapted for use on the real part of the FRF rather than the magnitude part.

Eqs. (4.4) and (4.5) are implicit in ψ and numerical solution is needed for obtaining the roots. Using the following approximation:

$$\sigma_\psi \cong 3\left(1 - \left(\frac{\psi}{\psi^{(1)}}\right)^4\right) \tag{4.6}$$

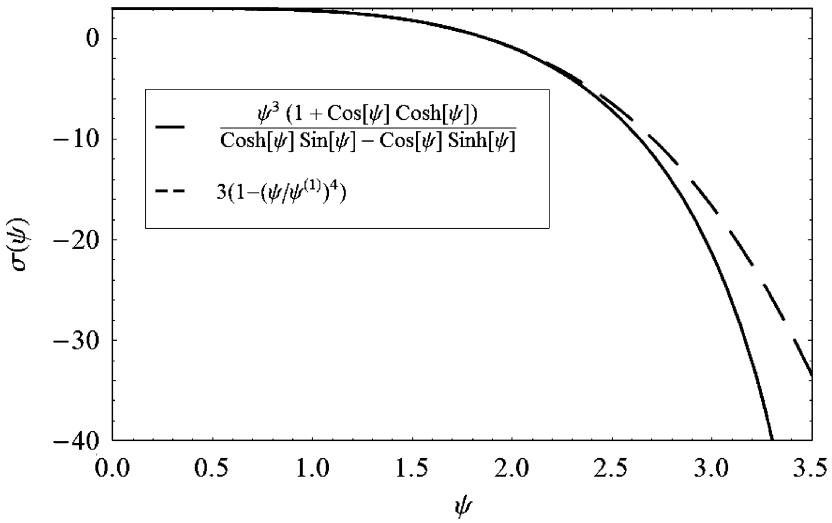

Fig. 8. Comparison of $\sigma(\psi)$ which controls $\psi^{(p)}$, $\psi^{(n)}$ and $\psi^{(a)}$, for continuous and lumped DVA systems. It is seen that for ψ up to 2.5 these functions are essentially the same.

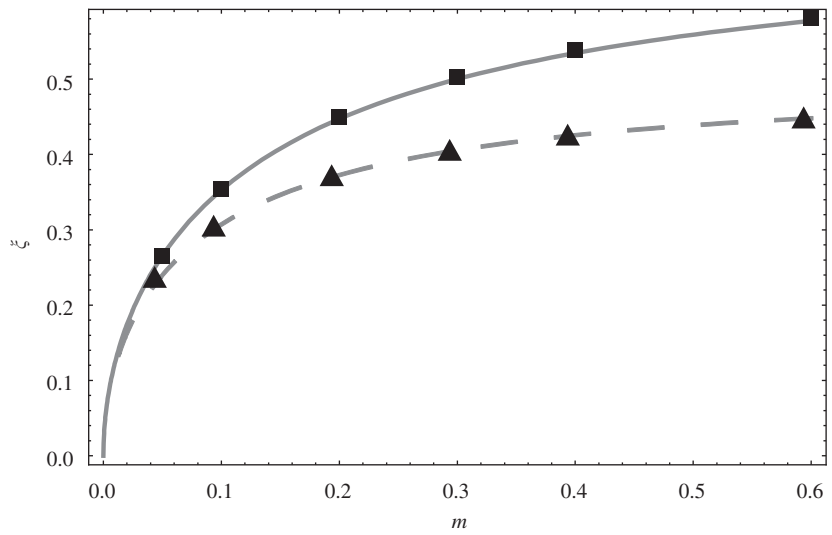

Fig. 9. DVA damping ratio (ξ) at optimal tuning for various values of mass ratios (m): – $\xi^{(p)}$ for lumped mass model, — $\xi^{(n)}$ for lumped mass model, ■ $\xi^{(p)}$ for the CDVA model and ▲ $\xi^{(n)}$ for the CDVA model.

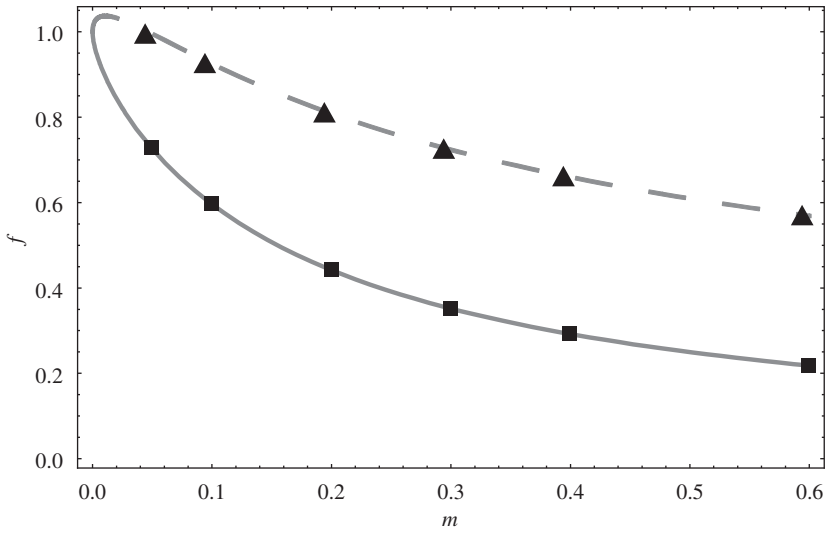

Fig. 10. DVA natural frequency (f) at optimal tuning for various values of mass ratios (m): – $f^{(p)}$ for lumped mass model, — $f^{(n)}$ for lumped mass model, ■ $f^{(p)}$ for continuous cantilever model and ▲ $f^{(n)}$ for continuous cantilever model.

and inserting into Eqs. (4.4) and (4.5), reduces to the corresponding equations given in Sims' work for the lumped system. Fig. 8 compares the exact and approximated σ_ψ from Eqs. (4.3) and (4.6). It can be concluded that lumped and continuous beams have essentially the same σ_ψ response for ψ up to 2.5.

In his work, Sims obtained the DVA damping ratio (ξ) and normalized eigen-frequency (f) at optimal tuning conditions for selected values of mass ratios (m). The parameters ξ and f are related to m, c and k by the following relations:

$$\xi = \frac{c}{2\sqrt{km}}; \quad f = (\psi^{(1)})^{-2}\sqrt{\frac{k}{m}} \tag{4.7}$$

Figs. 9 and 10 show ξ and f at optimal conditions for the lumped and continuous beam models. The curves represent the analytical solutions obtained by Sims while the points are related to the numerical solutions for the CDVA system. For maximizing $\min(\mathrm{Re}(G_1(i\omega)))$ ξ and f are denoted by $\xi^{(n)}$ and $f^{(n)}$ while for minimizing $\max(\mathrm{Re}(G_1(i\omega)))$ we use $\xi^{(p)}$ and $f^{(p)}$. It is shown that the two models yield approximately similar values for the optimal parameters. This is true as long as $\psi^{(p)}$, $\psi^{(n)}$ and $\psi^{(a)}$ are close to $\psi^{(1)}$.

5. Comparison of the VB with the CDVA system

The optimal response of the CDVA and VB systems will be compared in the following with respect to the three criteria discussed above: $\min(\mathrm{Re}(G_1(i\omega)))$, $\max(\mathrm{Re}(G_1(i\omega)))$ and $\mathrm{Abs}(G_1(i\omega))$.

Keeping the static stiffness constant, the FRF of the CDVA system is controlled by m, c and k, while E_1/E_2 and η control the FRF of the VB system.

As shown above, in the VB $\min(\mathrm{Re}(G_1(i\omega)))$ is optimized by tuning η for each E_1/E_2 ratio. In the CDVA system optimization is performed by tuning c and k for each m value; therefore, the mass ratio (m) in the CDVA system is equivalent to E_1/E_2 in the VB system. Fig. 11 shows $\mathrm{Re}(G_1(i\omega))$ for the two systems in their optimal response, having the same static stiffness and mass density. It is seen that increasing m or decreasing E_1/E_2 will always improve the optimal response (monotonic). Their limit will be controlled by design constraints.

One clear and important difference between the two systems is their $\max(\mathrm{Re}(G_1(i\omega)))$. This value becomes crucial when the cutting conditions are such that the sign of u_1 (3.1) changes. In this case the DVA modal parameters have to be tuned again for minimizing $\max(\mathrm{Re}(G_1(i\omega)))$. This is illustrated in Fig. 7 where for $m = 0.1$, $c = 0.1483$ and $k = 0.4413$, $\max(\mathrm{Re}(G_1(i\omega)))$ is optimized. On the other hand, we observe that in the

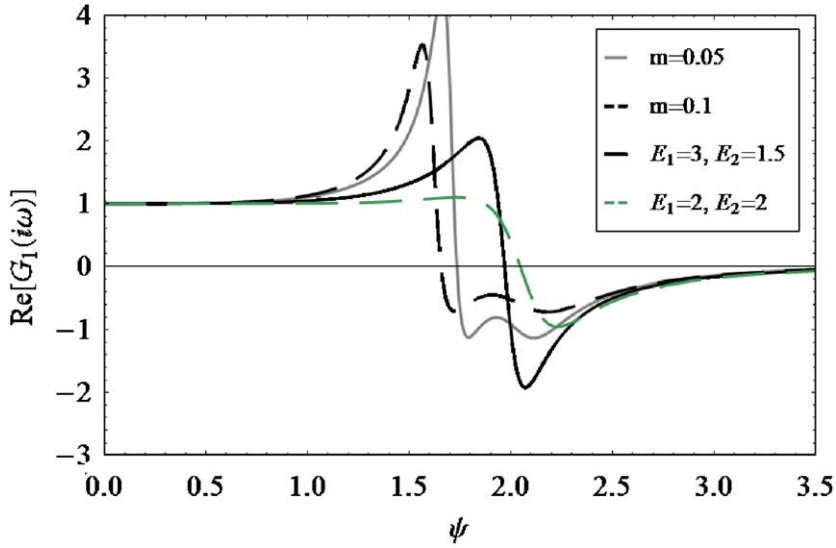

Fig. 11. Comparison of optimum frequency response function real part between DVA system and continuous viscoelastic cantilever. Static stiffness is similar.

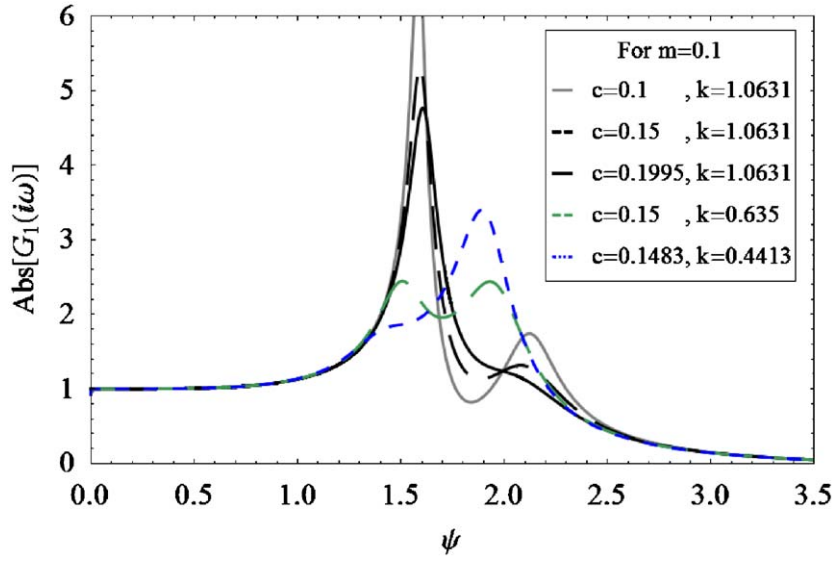

Fig. 12. The frequency response function magnitude, for a cantilever with DVA for several values of DVA modal parameters.

VB system (Fig. 4), max(Re(G_1(iω))) is close to the positive locked-point and therefore such re-tuning is not necessary.

In the general field of vibration control, it is often desirable to suppress Abs(G_1(iω)). Fig. 12 shows Abs(G_1(iω)) of the CDVA for the selected values of c and k above. It is found that Abs(G_1(iω)) is optimal when $c = 0.15$ and $k = 0.635$, according to Ormondroyd and Den Hartog's [15] "equal peaks" method.

In the CDVA system the optimal parameters for the above criteria are different: optimizing min(Re(G_1(iω))) leads to $c = 0.1995$, $k = 1.0631$, optimizing Abs(G_1(iω)) yields $c = 0.15$ and $k = 0.635$ and optimizing max(Re(G_1(iω))) leads to $c = 0.1483$ and $k = 0.4413$ (Figs. 7 and 12). On the other hand, the optimized VB system yields $\eta \cong 0.4$ for all these criteria (Figs. 13 and 4). The reason is that the peak of Abs(G_1(iω)) or max(Re(G_1(iω))) are close to the locked-points. This advantage was found to be valid for a wide range of E_1/E_2 ratios.

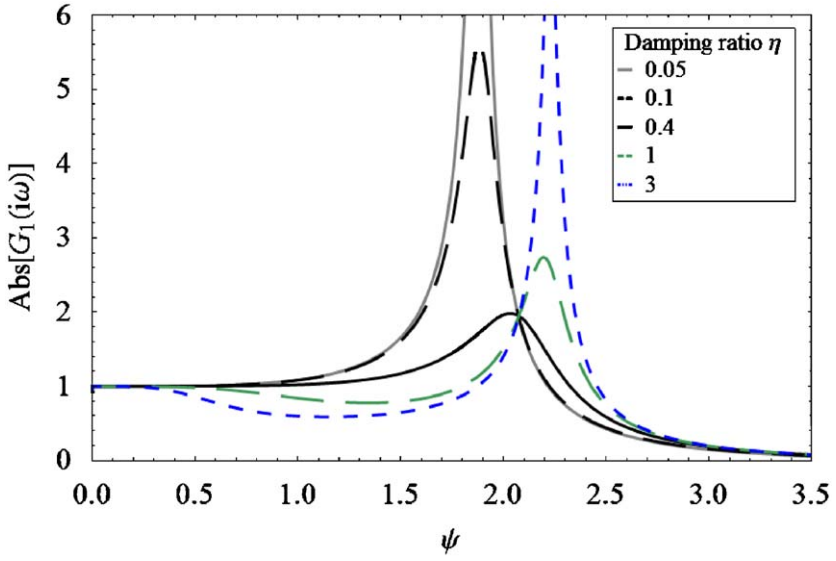

Fig. 13. The frequency response function magnitude, for a viscoelastic cantilever with $E_1 = E_2 = 2$ and various values of the damping ratio η.

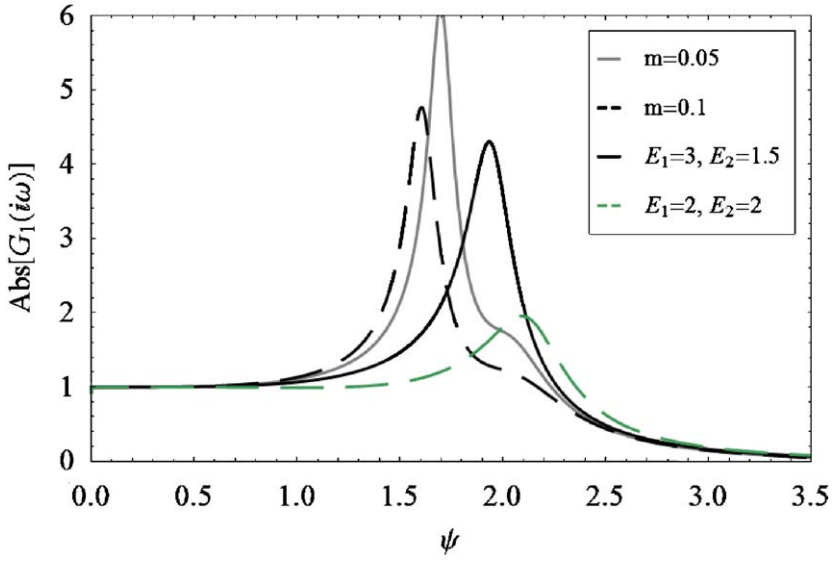

Fig. 14. Comparison of optimum frequency response function magnitude between DVA system and continuous viscoelastic cantilever. Static stiffness is similar.

We can draw a general conclusion with regard to the VB system. The parameters controlling the optimum performance for the three different stability criteria are approximately the same.

Examining the first resonant frequency for the two systems at the optimal parameters is also fruitful (Fig. 14). It is seen that improving the chatter resistance of the CDVA system by increasing m, is followed by a decrease in the resonant frequency which may undermine the optimization effect. On the other hand, in the optimized VB system, decreasing E_1/E_2 causes an increase in the resonant frequency, which strengthens the stability effect even further.

6. Conclusions

A viscoelastic beam for increasing the resistance against regenerative chatter of turning bars is analyzed and compared to the common DVA system. The structural viscoelastic material is modeled by a 3-parameter linear solid. The optimal chatter resistance is examined with respect to three stability measures: (1) the most negative real part of the FRF; (2) the most positive real part of the FRF and (3) the FRF peak magnitude in case of forced vibration. It was found that for the viscoelastic beam, all three measures are optimized near the same damping ratio. This result is difficult to achieve by a CDVA system since the DVA has to be tuned differently for each measure.

Optimal chatter resistance of the VB system is improved by decreasing the E_1/E_2 ratio while the CDVA system is improved by increasing the DVA mass ratio (m). An additional advantage of the VB is that increasing the optimal chatter resistance is followed by an increase in the resonant frequency, while decreasing it in the DVA system. Viscoelastic properties of a beam can be materialized by several techniques such as fluid surface damping, which is currently under investigation.

Acknowledgments

The authors gratefully acknowledge the partial support of ISCAR Company in Israel and the support of the Technion, Israel Institute of Technology.

References

[1] M. Wang, R. Fei, Chatter suppression based on nonlinear vibration characteristic of electrorheological fluids, *International Journal of Machine Tools and Manufacture* 39 (1999) 1925–1934.
[2] J. Tlusty, *Manufacturing Process and Equipment*, Prentice-Hall, NJ, 2000.
[3] J.R. Pratt, A.H. Nayfeh, Chatter control and stability analysis of a cantilever boring bar under regenerative cutting conditions, *Philosophical Transactions of the Royal Society of London, Part A* 359 (2001) 759–792.
[4] C.K. Chen, Y.M. Tsao, A stability analysis of regenerative chatter in turning process without using tailstock, *International Journal of Advanced Manufacturing Technology* 29 (2006) 648–654.
[5] T. Takemura, T. Kitamura, T. Hoshi, K. Okushima, Active suppression of chatter by programmed variation of spindle speed, *Annals of the International Institute for Production Engineering Research* 23 (1974) 121–122.
[6] J.R. Pratt, A.H. Nayfeh, Design and modeling for chatter control, *Nonlinear Dynamics* 19 (1999) 49–69.
[7] S.A. Tobias, *Machine–Tool Vibration*, Wiley, New York, 1965.
[8] E.I. Rivin, H. Kang, Enhancement of dynamic stability of cantilever tooling structures, *International Journal of Machine Tools and Manufacture* 32 (1992) 539–561.
[9] M.D. Thomas, W.A. Knmight, M.M. Sadek, Comparative dynamic performance of boring bars, *Proceedings of 11th International MTDR Conference*, Pergamon Press, Oxford, 1970.
[10] G.N. Meshcheriakov, L.P. Tuscharova, N.G. Meshcheriakov, A.N. Sivakov, Machine tool vibration stability depending on adjustment of dominant stiffness axes, *Annals of CIRP* 33 (1984) 271–272.
[11] S. Nagano, T. Koizumi, T. Fujii, N. Tsujiuchi, H. Ueda, K. Steel, Development of a composite boring bar, *Composite Structures* 38 (1–4) (1997) 531–539.
[12] E.I. Rivin, H. Kang, Improvement of machining conditions for slender parts by tuned dynamic stiffness of tool, *International Journal of Machine Tools and Manufacture* 29 (1989) 361–376.
[13] J. Donies, L. Van Den Noortgate, *Machining of Deep Holes without Chatter. Note Technique 10*, Crif, Belgium, 1974.
[14] E.I. Rivin, An extra-long cantilever boring bar with enhanced chatter resistance, *Proceedings of 15th North American Manufacturing Research Conference SME*, 1987, pp. 447–452.
[15] J.P. Den Hartog, *Mechanical Vibrations*, fourth ed., McGraw-Hill, New York, 1956.
[16] N.D. Sims, Vibration absorbers for chatter suppression: a new analytical tuning methodology, *Journal of Sound and Vibration* 301 (2007) 592–607.
[17] J.K. Liu, K.E. Rouch, Optimal passive vibration control of cutting process stability in milling, *Journal of Materials Processing Technology* 28 (1–2) (1991) 285–294.
[18] Y.S. Tarng, J.Y. Kao, E.C. Lee, Chatter suppression in turning operations with a tuned vibration absorber, *Journal of Materials Processing Technology* 105 (1) (2000) 55–60.
[19] E.I. Rivin, *Stiffness and Damping in Mechanical Design*, Marcel Dekker, New York, 1999.
[20] H. Ghoneim, Fluid surface damping: a technique for vibration suppression of beams, *Shock and Vibration* 4 (1997) 295–304.
[21] J. Tlusty, M. Polacek, The stability of the machine tool against self excited vibration in machining, *Proceedings of the Production Engineering Research Conference on ASME*, Pittsburgh, 1963.

[22] I. Karnovsky, O. Lebed, *Formulas for Structural Dynamics: Tables, Graphs and Solutions*, McGraw-Hill, New York, 2001.
[23] W. Flügge, *Viscoelasticity*, second ed., Springer, New York, 1975.
[24] P. Szuba, Q. Zou, G.C. Barber, L. Yang, Optimization of hollow cantilevered boring bar stiffness, *Machining Science and Technology* 9 (3) (2005) 325–343.
[25] K. Yen, W. Hsueh, Suppression of chatter vibration in inner-diameter cutting, *JSME International Journal Series C: Dynamics, Control, Robotics and Design Manufacturing* 39 (1996) 25–33.
[26] B.G. Korenev, L.M. Reznikov, *Dynamic Vibration Absorbers*, Wiley, England, 1993.